NUREG/CR-5926
MEA-2490

SANS Investigation of Low Alloy Steels in Neutron Irradiated, Annealed, and Reirradiated Conditions

Prepared by
R. Kampmann, F. Frisius, H. Hackbarth, P. A. Beaven, R. Wagner/IMR-GKSS
J. R. Hawthorne/MEA

Institute for Materials Research
GKSS – Research Center

Materials Engineering Associates, Inc.

Prepared for
U.S. Nuclear Regulatory Commission

AVAILABILITY NOTICE

Availability of Reference Materials Cited in NRC Publications

Most documents cited in NRC publications will be available from one of the following sources:

1. The NRC Public Document Room, 2120 L Street, NW., Lower Level, Washington, DC 20555

2. The Superintendent of Documents, U.S. Government Printing Office, P.O. Box 37082, Washington, DC 20013-7082

3. The National Technical Information Service, Springfield, VA 22161

Although the listing that follows represents the majority of documents cited in NRC publications, it is not intended to be exhaustive.

Referenced documents available for inspection and copying for a fee from the NRC Public Document Room include NRC correspondence and internal NRC memoranda; NRC bulletins, circulars, information notices, inspection and investigation notices; licensee event reports; vendor reports and correspondence; Commission papers; and applicant and licensee documents and correspondence.

The following documents in the NUREG series are available for purchase from the GPO Sales Program: formal NRC staff and contractor reports, NRC-sponsored conference proceedings, international agreement reports, grant publications, and NRC booklets and brochures. Also available are regulatory guides, NRC regulations in the *Code of Federal Regulations*, and *Nuclear Regulatory Commission Issuances*.

Documents available from the National Technical Information Service include NUREG-series reports and technical reports prepared by other Federal agencies and reports prepared by the Atomic Energy Commission, forerunner agency to the Nuclear Regulatory Commission.

Documents available from public and special technical libraries include all open literature items, such as books, journal articles, and transactions. *Federal Register* notices, Federal and State legislation, and congressional reports can usually be obtained from these libraries.

Documents such as theses, dissertations, foreign reports and translations, and non-NRC conference proceedings are available for purchase from the organization sponsoring the publication cited.

Single copies of NRC draft reports are available free, to the extent of supply, upon written request to the Office of Administration, Distribution and Mail Services Section, U.S. Nuclear Regulatory Commission, Washington, DC 20555.

Copies of industry codes and standards used in a substantive manner in the NRC regulatory process are maintained at the NRC Library, 7920 Norfolk Avenue, Bethesda, Maryland, for use by the public. Codes and standards are usually copyrighted and may be purchased from the originating organization or, if they are American National Standards, from the American National Standards Institute, 1430 Broadway, New York, NY 10018.

DISCLAIMER NOTICE

NUREG/CR-5926
MEA-2490

SANS Investigation of Low Alloy Steels in Neutron Irradiated, Annealed, and Reirradiated Conditions

Prepared by
R. Kampmann, F. Frisius, H. Hackbarth, P. A. Beaven, R. Wagner/IMR-GKSS
J. R. Hawthorne/MEA

Institute for Materials Research
GKSS – Research Center

Materials Engineering Associates, Inc.

Prepared for
U.S. Nuclear Regulatory Commission

AVAILABILITY NOTICE

Availability of Reference Materials Cited in NRC Publications

Most documents cited in NRC publications will be available from one of the following sources:

1. The NRC Public Document Room, 2120 L Street, NW., Lower Level, Washington, DC 20555

2. The Superintendent of Documents, U.S. Government Printing Office, P.O. Box 37082, Washington, DC 20013-7082

3. The National Technical Information Service, Springfield, VA 22161

Although the listing that follows represents the majority of documents cited in NRC publications, it is not intended to be exhaustive.

Referenced documents available for inspection and copying for a fee from the NRC Public Document Room include NRC correspondence and internal NRC memoranda; NRC bulletins, circulars, information notices, inspection and investigation notices; licensee event reports; vendor reports and correspondence; Commission papers; and applicant and licensee documents and correspondence.

The following documents in the NUREG series are available for purchase from the GPO Sales Program: formal NRC staff and contractor reports, NRC-sponsored conference proceedings, international agreement reports, grant publications, and NRC booklets and brochures. Also available are regulatory guides, NRC regulations in the *Code of Federal Regulations*, and *Nuclear Regulatory Commission Issuances*.

Documents available from the National Technical Information Service include NUREG-series reports and technical reports prepared by other Federal agencies and reports prepared by the Atomic Energy Commission, forerunner agency to the Nuclear Regulatory Commission.

Documents available from public and special technical libraries include all open literature items, such as books, journal articles, and transactions. *Federal Register* notices, Federal and State legislation, and congressional reports can usually be obtained from these libraries.

Documents such as theses, dissertations, foreign reports and translations, and non-NRC conference proceedings are available for purchase from the organization sponsoring the publication cited.

Single copies of NRC draft reports are available free, to the extent of supply, upon written request to the Office of Administration, Distribution and Mail Services Section, U.S. Nuclear Regulatory Commission, Washington, DC 20555.

Copies of industry codes and standards used in a substantive manner in the NRC regulatory process are maintained at the NRC Library, 7920 Norfolk Avenue, Bethesda, Maryland, for use by the public. Codes and standards are usually copyrighted and may be purchased from the originating organization or, if they are American National Standards, from the American National Standards Institute, 1430 Broadway, New York, NY 10018.

NUREG/CR-5926
MEA-2490
RF, R5

SANS Investigation of Low Alloy Steels in Neutron Irradiated, Annealed, and Reirradiated Conditions

Manuscript Completed: January 1993
Date Published: February 1993

Prepared by
R. Kampmann, F. Frisius, H. Hac. arth, P. A. Beaven, R. Wagner, Institute for Materials Research, GKSS
J. R. Hawthorne, Materials Engine ing Associates, Inc.

Institute for Materials Research
GKSS - Research Center
P.O. Box 1160
2054 Geesthacht, Germany

Under Contract to:
Materials Engineering Associates, Inc.
9700-B Martin Luther King, Jr. Highway
Lanham, MD 20706-1837

Prepared for
Division of Engineering
Office of Nuclear Regulatory Research
U.S. Nuclear Regulatory Commission
Washington, DC 20555
NRC FIN B5848

ABSTRACT

Small Angle Neutron Scattering (SANS) experiments were made on several low alloy steels and submerged-arc welds prototypic of nuclear reactor vessel construction. The objective was the characterization of radiation-enhanced and/or radiation-induced precipitation contributing to mechanical property changes observed in tensile and notch ductility tests of the materials. The materials were irradiated in the UBR Test Reactor under closely controlled conditions.

A portion of the samples were examined in the 288°C irradiated (I) condition; others were examined in the postirradiation annealed (IA) condition and in the 288°C reirradiated (IAR) condition. Experimental variables included material composition (primarily %Cu, %P, %Ni content), postirradiation annealing temperature (454°C and 399°C), reirradiation fluence level, and neutron-fluence rate (~0.08, 0.7, and 9×10^{12} $n/cm^2\text{-}s^{-1}$, $E > 1$ MeV). The apparent influence of the described variables on the size, number density, and composition of copper-rich precipitates was the primary focus of the SANS analyses. SANS observations are related to measured notch ductility and tensile property changes, with a view toward mechanistic explanation of the observed mechanical property trends for I, IA, and IAR conditions.

CONTENTS

LIST OF FIGURES

LIST OF TABLES

FOREWORD

The work reported here was performed at Materials Engineering Associates (MEA) under the program, Irradiation Embrittlement of Reactor Pressure Vessel Steels, F. J. Loss, Program Manager. The program is sponsored by the Office of Nuclear Regulatory Research of the U. S. Nuclear Regulatory Commission (NRC). The technical monitor for the NRC is E. M. Hackett.

Reports under the prior contract, Structural Integrity of Water Reactor Pressure Boundary Components, are listed below:

1. J. R. Hawthorne, "Significance of Nickel and Copper Content to Radiation Sensitivity and Postirradiation Heat Treatment Recovery of Reactor Vessel Steels," USNRC Report NUREG/CR-2948, Nov. 1982.

2. "Structural Integrity of Water Reactor Pressure Boundary Components, Annual Report for 1982," F. J. Loss, Ed., USNRC Report NUREG/CR-3228, Vol. 1, Apr. 1983.

3. J. R. Hawthorne, "Exploratory Assessment of Postirradiation Heat Treatment Variables in Notch Ductility Recovery of A 533-B Steel," USNRC Report NUREG/CR-3229, Apr. 1983.

4. W. H. Cullen, K. Torronen, and M. Kemppainen, "Effects of Temperature on Fatigue Crack Growth of A 508-2 Steel in LWR Environment," USNRC Report NUREG/CR-3230, Apr. 1983.

5. "Proceedings of the International Atomic Energy Agency Specialists' Meeting on Subcritical Crack Growth," Vols. 1 and 2, W. H. Cullen, Ed., USNRC Conference Proceeding NUREG/CP-0044, May 1983.

6. W. H. Cullen, "Fatigue Crack Growth Rates of A 508-2 Steel in Pressurized, High-Temperature Water," USNRC Report NUREG/CR-3294, June 1983.

7. J. R. Hawthorne, B. H. Menke, and A. L. Hiser, "Light Water Reactor Pressure Vessel Surveillance Dosimetry Improvement Program: Notch Ductility and Fracture Toughness Degradation of A 302-B and A 533-B Reference Plates from PSF Simulated Surveillance and Through-Wall Irradiation Capsules," USNRC Report NUREG/CR-3295, Vol. 1, Apr. 1984.

8. J. R. Hawthorne and B. H. Menke, "Light Water Reactor Pressure Vessel Surveillance Dosimetry Improvement Program: Postirradiation Notch Ductility and Tensile Strength Determinations for PSF Simulated Surveillance and Through-Wall Specimen Capsules," USNRC Report NUREG/CR-3295, Vol. 2, Apr. 1984.

9. A. L. Hiser and F. J. Loss, "Alternative Procedures for J-R Curve Determination," USNRC Report NUREG/CR-3402, July 1983.

10. A. L. Hiser, F. J. Loss, and B. H. Menke, "J-R Curve Characterization of Irradiated Low Upper Shelf Welds," USNRC Report NUREG/CR-3506, Apr. 1984.

11. W. H. Cullen, R. E. Taylor, K. Torronen, and M. Kemppainen, "The Temperature Dependence of Fatigue Crack Growth Rates of A 351 CF8A Cast Stainless Steel in LWR Environment," USNRC Report NUREG/CR-3546, Apr. 1984.

12. "Structural Integrity of Light Water Reactor Pressure Boundary Components -- Four-Year Plan 1984-1988," F. J. Loss, Ed., USNRC Report NUREG/CR-3788, Sep. 1984.

13. W. H. Cullen and A. L. Hiser, "Behavior of Subcritical and Slow-Stable Crack Growth Following a Postirradiation Thermal Anneal Cycle," USNRC Report NUREG/CR-3833, Aug. 1984.

14. "Structural Integrity of Water Reactor Pressure Boundary Components: Annual Report for 1983," F. J. Loss, Ed., USNRC Report NUREG/CR-3228, Vol. 2, Sept. 1984.

15. W. H. Cullen, "Fatigue Crack Growth Rates of Low-Carbon and Stainless Piping Steels in PWR Environment," USNRC Report NUREG/CR-3945, Feb. 1985.

16. W. H. Cullen, M. Kemppainen, H. Hanninen, and K. Torronen, "The Effects of Sulfur Chemistry and Flow Rate on Fatigue Crack Growth Rates in LWR Environments," USNRC Report NUREG/CR-4121, Feb. 1985.

17. "Structural Integrity of Water Reactor Pressure Boundary Components: Annual Report for 1984," F. J. Loss, Ed., USNRC Report NUREG/CR-3228, Vol. 3, June 1985.

18. A. L. Hiser, "Correlation of C_v and K_{Ic}/K_{Jc} Transition Temperature Increases Due to Irradiation," USNRC Report NUREG/CR-4395, Nov. 1985.

19. W. H. Cullen, G. Gabetta, and H. Hanninen, "A Review of the Models and Mechanisms For Environmentally-Assisted Crack Growth of Pressure Vessel and Piping Steels in PWR Environments," USNRC Report NUREG/CR-4422, Dec. 1985.

20. "Proceedings of the Second International Atomic Energy Agency Specialists' Meeting on Subcritical Crack Growth," W. H. Cullen, Ed., USNRC Conference Proceeding NUREG/CP-0067, Vols. 1 and 2, Apr. 1986.

21. J. R. Hawthorne, "Exploratory Studies of Element Interactions and Composition Dependencies in Radiation Sensitivity Development," USNRC Report NUREG/CR-4437, Nov. 1985.

22. R. B. Stonesifer and E. F. Rybicki, "Development of Models for Warm Prestressing," USNRC Report NUREG/CR-4491, Jan. 1987.

23. E. F. Rybicki and R. B. Stonesifer, "Computational Model for Residual Stresses in a Clad Plate and Clad Fracture Specimens," USNRC Report NUREG/CR-4635, Oct. 1986.

24. D. E. McCabe, "Plan for Experimental Characterization of Vessel Clad Steel After Irradiation," USNRC Report NUREG/CR-4636, Oct. 1986.

25. E. F. Rybicki, J. R. Shadley, and A. S. Sandhu, "Experimental Evaluation of Residual Stresses in a Weld Clad Plate and Clad Test Specimens," USNRC Report NUREG/CR-4646, Oct. 1986.

26. "Structural Integrity of Water Reactor Pressure Boundary Components: Annual Report for 1985," F. J. Loss, Ed., USNRC Report NUREG/CR-3228, Vol. 4, June 1986.

27. G. Gabetta and W. H. Cullen, "Application of a Two-Mechanism Model for Environmentally-Assisted Crack Growth," USNRC Report NUREG/CR-4723, Oct. 1986.

28. W. H. Cullen, "Fatigue Crack Growth Rates in Pressure Vessel and Piping Steels in LWR Environments," USNRC Report NUREG/CR-4724, Mar. 1987.

29. W. H. Cullen and M. R. Jolles, "Fatigue Crack Growth of Part-Through Cracks in Pressure Vessel and Piping Steels: Air Environment Results, USNRC Report NUREG/CR-4828, Oct. 1988.

30. D. E. McCabe, "Fracture Evaluation of Surface Cracks Embedded in Reactor Vessel Cladding: Unirradiated Bend Specimen Results," USNRC Report NUREG/CR-4841, May 1987.

31. H. Hanninen, M. Vulli, and W. H. Cullen, "Surface Spectroscopy of Pressure Vessel Steel Fatigue Fracture Surface Films Formed in PWR Environments," USNRC Report NUREG/CR-4863, July 1987.

32. A. L. Hiser and G. M. Callahan, "A User's Guide to the NRC's Piping Fracture Mechanics Data Base (PIFRAC)," USNRC Report NUREG/CR-4894, May 1987.

33. "Proceedings of the Second CSNI Workshop on Ductile Fracture Test Methods (Paris, France, April 17-19, 1985)," F. J. Loss, Ed., USNRC Conference Proceeding NUREG/CP-0064, Aug, 1988.

34. W. H. Cullen and D. Broek, "The Effects of Variable Amplitude Loading on A 533-B Steel in High-Temperature Air and Reactor Water Environments," USNRC Report NUREG/CR-4929, Apr. 1989.

35. "Structural Integrity of Water Reactor Pressure Boundary Components: Annual Report for 1986," F. J. Loss, Ed., USNRC Report NUREG/CR-3228, Vol. 5, July 1987.

36. F. Ebrahimi, et al., "Development of a Mechanistic Understanding of Radiation Embrittlement in Reactor Pressure Vessel Steels: Final Report," USNRC Report NUREG/CR-5063, Jan. 1988.

37. J. B. Terrell, "Fatigue Life Characterization of Smooth and Notched Piping Steel Specimens in 288°C Air Environments," USNRC Report NUREG/CR-5013, May 1988.

38. A. L. Hiser, "Tensile and J-R Curve Characterization of Thermally Aged Cast Stainless Steels," USNRC Report NUREG/CR-5024, Sept. 1988

39. J. B. Terrell, "Fatigue Strength of Smooth and Notched Specimens of ASME SA 106-B Steel in PWR Environments," USNRC Report NUREG/CR-5136, Sept. 1988.

40. D. E. McCabe, "Fracture Evaluation of Surface Cracks Embedded in Reactor Vessel Cladding: Material Property Evaluations" USNRC NUREG/CR-5207, Sept. 1988.

41. J. R. Hawthorne and A. L. Hiser, "Experimental Assessments of Gundremmingen RPV Archive Material for Fluence Rate Effects Studies," USNRC Report NUREG/CR-5201, Oct. 1988.

42. J. B. Terrell, "Fatigue Strength of ASME SA 106-B Welded Steel Pipes in 288°C Air Environments," USNRC Report NUREG/CR-5195, Dec. 1988.

43. A. L. Hiser, "Post-Irradiation Fracture Toughness Characterization of Four Lab-Melt Plates," USNRC Report NUREG/CR-5216, Rev. 1, June 1989.

44. R. B. Stonesifer, E. F. Rybicki, and D. E. McCabe, "Warm Prestress Modeling: Comparison of Models and Experimental Results," USNRC Report NUREG/CR-5208, Apr. 1989.

45. A. L. Hiser and J. B. Terrell, "Size Effects on J-R Curves for A 302-B Plate," USNRC Report NUREG/CR-5265, Jan. 1989.

46. D. E. McCabe, "Fracture Evaluation of Surface Cracks Embedded in Reactor Vessel Cladding," USNRC Report NUREG/CR-5326, Mar. 1989.

47. J. R. Hawthorne, "An Exploratory Study of Element Interactions and Composition Dependencies in Radiation Sensitivity Development: Final Report," USNRC Report NUREG/CR-5357, Apr. 1989

48. J. R. Hawthorne, "Steel Impurity Element Effects on Postirradiation Properties Recovery by Annealing: Final Report," USNRC Report NUREG/CR-5388, Aug. 1989.

49. J. R. Hawthorne, "Irradiation-Anneal-Reirradiation (IAR) Studies of Prototypic Reactor Vessel Weldments," USNRC Report NUREG/CR-5469, Nov. 1989.

50. J. R. Hawthorne and A. L. Hiser, "Invescigations of Irradiation-Anneal-Reirradiation (IAR) Properties Trends of RPV Welds: Phase 2 Final Report," USNRC Report NUREG/CR-5492, Jan. 1990.

51. H. H. Hanninen and W. H. Cullen, "Slow Strain Rate Testing of a Cyclically Stabilized A-516 Gr. 70 Piping Steel in PWR Conditions," USNRC Report NUREG/CR-5327, Nov. 1989.

52. A. L. Hiser, "Fracture Toughness Characterization of Nuclear Piping Steels," USNRC Report NUREG/CR-5188, Nov. 1989.

53. J. R. Hawthorne and A. L. Hiser, "Influence of Fluence Rate on Radiation-Induced Mechanical Property Changes in Reactor Pressure Vessel Steels," USNRC Report NUREG/CR-5493, Mar. 1990.

54. A. L. Hiser, "Correlation of Irradiation-Induced Transition Temperature Increases from C_v and K_{Jc}/K_{Ic} Data," USNRC Report NUREG/CR-5494, Mar. 1990.

55. J. R. Hawthorne, "Accelerated Irradiation Test of Gundremmingen Reactor Vessel Trepan Material," USNRC Report NUREG/CR-5891, August 1992.

Prior reports dealing with the specific topic of this report are listed below:

J. R. Hawthorne and A. L. Hiser, "Investigations of Irradiation-Anneal-Reirradiation (IAR) Properties Trends of RPV Welds: Phase 2 Final Report," USNRC Report NUREG/CR-5492, Jan. 1990.

J. R. Hawthorne, "Steel Impurity Element Effects on Postirradiation Properties Recovery by Annealing: Final Report," USNRC Report NUREG/CR-5388, Aug. 1989.

J. R. Hawthorne, "An Exploratory Study of Element Interactions and Composition Dependencies in Radiation Sensitivity Development: Final Report," USNRC Report NUREG/CR-5357, Apr. 1989

P. A. Beaven, F. Frisius, R. Kampmann, R. Wagner, and J. R. Hawthorne, "SANS Investigation of Irradiated A 533-B Steels Doped with Phosphorus," in Radiation Embrittlement of Nuclear Reactor Pressure Vessel Steels: An International Review, L. E. Steele, Ed., ASTM STP 1011, Vol. 3, American Society for Testing and Materials, Philadelphia, PA, 1989, p. 243.

F. Ebrahimi, et al., "Development of a Mechanistic Understanding of Radiation Embrittlement in Reactor Pressure Vessel Steels: Final Report," USNRC Report NUREG/CR-5063, Jan. 1988.

1. INTRODUCTION

The sensitivity of pressure vessel steels to 288°C neutron irradiation embrittlement depends especially on steel composition, neutron fluence, fluence rate, annealing, and reirradiation conditions. The correlation of the microstructural changes due to the irradiation and annealing procedures with the deterioration of the mechanical properties is the basis for elucidating the mechanisms of irradiation embrittlement (Refs. 1 and 2).

Due to the small size of radiation-induced defects present in ferritic steels of complicated microstructure it is extremely difficult to analyze them by means of Transmission Electron Microscopy (TEM) (Ref. 3). The rather small number density of the defects strongly impedes their statistical analysis by means of atom-probe field ion microscopy (AP/FIM). Nevertheless, direct observations of defect sizes and compositions have been achieved using this techn [illegible] (Ref. 4) The results agree with those of the SANS studies. The S[illegible] technique has most successfully been applied to analyze defect microstructures in ferritic steels. The results are representative for large sample volumes and defect sizes; number densities and volume fractions can be determined with considerable accuracy. Very small defects of diameters even smaller than 1 nm can be analyzed; from the relative strength of the magnetic and the nuclear scattering contributions, important conclusions concerning the composition of defects can be drawn. In particular, SANS studies of RPV steels have revealed that the irradiation-induced defects in RPV steels are neither simple voids nor pure Cu precipitates (Refs. 5, 6, 7, and 8).

The present SANS investigation is concerned with the characterization of defects formed in plates from commercial and laboratory melts, and weld deposits of low alloy steels during fast neutron irradiation, annealing, and reirradiation treatments. Experimental variables include fluence levels during irradiation and reirradiation, fluence rate, temperature of postirradiation annealing, and material composition.

2. EXPERIMENTAL DETAILS

2.1 Materials and Irradiation

The SANS specimens of 2 cm x 1 cm x 1 cm size were cut from broken halves of Charpy V-notch specimens. Weld deposits (Codes W8A, W9A, and WW7), plates of low alloy steels (Codes 23F and 23G), and plates from laboratory melts (Codes 68A, 68B, and 68C) have been studied. The chemical compositions of the materials are given in Table 1. The irradiation (I), annealing (IA), and reirradiation (IAR) treatments of the samples are given in Table 2. The plates were analyzed only in the I condition, the laboratory melts in the I and IA condition, and the welds in the I and IAR conditions. I-condition treatments include fluences between 0.45 and 3.85 x 10^{19} n/cm^2 and neutron fluence rates between 0.08 and 9 x 10^{12} n/cm^2-s^{-1}. Irradiated samples were annealed for 168 h at 399°C or 454°C. Fluences of 0.37 and 1.12 x 10^{19} n/cm^2 were applied during reirradiations. All irradiation and reirradiation treatments were performed at 288°C.

2.2 SANS Measurements

SANS experiments were performed at the new SANS-2 facility at the FRG-1 research reactor in Geesthacht/FRG, which was put into operation in Spring 1990. A neutron beam with a mean wavelength of 5.25 Å and a half-width of 11.5% was used. The specimens were investigated in pairs (irradiated and unirradiated as reference) to enable the difference in SANS intensity resulting from the I, IA, or IAR treatments to be measured. During the measurements, the samples were magnetized by a strong magnetic field parallel to their long dimension (internal magnetic field ≅ 13k Oersted). In this way, the magnetization of the sample was aligned into a horizontal direction perpendicular to the neutron beam. The scattering intensity was measured as a function of the scattering angle by means of position-sensitive detectors parallel and perpendicular to the applied magnetic field. By placing the detectors at distances of ~ 90 cm and ~ 290 cm, the entire range of relevant scattering vectors could be covered. The detectors were calibrated using a vanadium sample.

2.3 SANS Interpretation

The defects giving rise to SANS are assumed to be three dimensional. This was already inferred from specific features of the SANS curves in former studies and, in some cases, was also confirmed by complementary techniques such as TEM (Ref. 3) or AP/FIM (Ref. 4). The SANS intensity arising from planar dislocation loops is supposed to be negligibly small.

The SANS interpretation procedure is analogous to the one described in a former paper (Ref. 2). The defects which might be voids, Cu precipitates or Cu-rich clusters are not ferromagnetic. Thus the difference of the magnetic scattering length density between the defects and the matrix $\Delta\eta_{mag}$ is independent of the composition of the

Table 1 Material Compositions

Material	Chemical Composition (wt%)									Remarks
	C	Mn	P	S	Si	Cu	Ni	Cr	Mo	
Weld No. 1 (min)	0.079	1.27	0.010	0.012	0.71	0.37	0.55	0.10	0.42	Linde 80 welding flux
(Code W8A) (max)	0.096	1.36	0.017	0.019	0.79	0.42	0.68	0.13	0.50	
Weld No. 2 (min)	0.19	1.21	0.008	0.005	0.23	0.35	0.64	0.10	0.49	Linde 0091 welding
(Code W9A) (max)	0.19	1.27	0.012	0.010	0.23	0.43	0.77	0.11	0.50	flux; used same filler wire lot as Weld W8A
Weld No. 3 (Code WW7)	0.08	1.56	0.013	0.008	0.60	0.35	0.10	0.12	0.54	Linde 80 welding flux
Plate 23F	0.23	1.35	0.015	0.021	0.22	0.21	0.22	0.12	0.52	ASTM A 302-B Ref. Plate
Plate 23G	0.22	1.40	0.017	0.008	0.19	0.20	0.63	0.20	0.54	MEA A 533-B Ref. Plate
Plate 68A	0.23	1.31	0.003	0.017	0.22	0.30	0.70	<0.003	0.52	Laboratory Melt 68, Cast A
Plate 68C	0.23	1.31	0.028	0.017	0.22	0.30	0.70	<0.003	0.52	Laboratory Melt 68, Cast C
Plate 67C	0.23	1.31	0.025	0.018	0.20	0.002	0.70	<0.003	0.51	Laboratory Melt 67, Cast C

Table 2 Irradiation (I), Annealing (IA), and Reirradiation (IAR) Treatments of Samples (Irradiation Temperature 288°C)

Material Condition	Irradiation		Annealing		Reirradiation		Weld[c]			Plate[c]		Lab. Melt[c]		
	Fluence[a]	Fluence[b] Rate	Temp (°C)	Time (h)	Fluence[a]	Fluence[b] Rate	W8A	W9A	WW7	23F	23G	68A	68C	67C
I-1	0.45	9	---	---	----	-	-	-	-	-	X	-	-	-
I-2	0.56	9	---	---	----	-	X	-	-	X	-	-	-	-
I-3	0.54	0.08	---	---	----	-	-	-	-	X	X	-	-	-
I-4	1.44	9	---	---	----	-	X	X	X	-	-	-	-	-
I-5	2.23	9	---	---	----	-	X	-	-	X	-	-	-	-
I-6	3.85	0.7	---	---	----	-	X	-	-	X	-	-	-	-
I-7	2.5	9	---	---	----	-	-	-	-	-	-	Z	Z	Z
IA-1	2.5	9	454	168	----	-	-	-	-	-	-	Z	Z	-
IA-2	2.5	9	399	168	----	-	-	-	-	-	-	X	X	X
IAR-1	1.44	9	399	168	0.37	9	X	X	X	-	-	-	-	-
IAR-2	1.44	9	399	168	1.09	9	X	-	X	-	-	-	-	-
IAR-3	1.44	9	4[illegible]	168	0.37	9	X	-	X	-	-	-	-	-
IAR-4	1.44	9	454	168	1.12	9	X	X	X	-	-	-	-	-

[a] x 10^{19} n/cm^2 E > 1 MeV [b] x 10^{12} n/cm^2-s^{-1} [c] X = this study; Z = previous study (Ref. 2)

defects ($\Delta\eta_{mag} = \eta^{m}_{mag}$; m refers to the matrix), whereas the corresponding nuclear "scattering contrast," $\Delta\eta_{nuc}$, is determined by the relative matrix and defect compositions.

Such non-ferromagnetic clusters embedded in a ferromagnetic matrix give rise to a SANS cross section $d\Sigma/d\Omega$ which is composed of nuclear $d\Sigma_{nuc}/d\Omega$ and magnetic $d\Sigma_{mag}/d\Omega$ scattering contributions both of which depend in the same manner on the defect volume fraction f and their specific structure factors F(h(R);s(κR)):

$$\frac{d\Sigma(\kappa,\alpha)}{d\Omega} = f(1-f)\left[(\Delta\eta_{nuc})^2+(\eta^{m}_{mag})^2\sin^2\alpha\right]F\left(h(R);s(\kappa R)\right) \qquad (1)$$

where

α = angle between the scattering vector κ and the magnetization of the sample

κ = $|\vec{\kappa}| = 4\pi\sin(\theta/2)/\lambda$

θ = scattering angle

λ = neutron wavelength.

Only the magnetic scattering contribution depends on the angle α and can therefore be separated from the nuclear one by measuring the SANS intensity parallel ($d\Sigma^{||}/d\Omega = d\Sigma_{nuc}/d\Omega$) and perpendicular ($d\Sigma^{\perp}/d\Omega = d\Sigma_{mag}(\alpha=90^{\circ})/d\Omega + d\Sigma_{nuc}/d\Omega$) to the magnetization of the sample.

We assumed the precipitates or voids formed during irradiation or annealing to be of spherical shape. Their size distributions were approximated by logarithmic normal distributions with fitting parameters R and p, i.e., determining the mean size and the width of the distribution. The corresponding mathematical expressions for $s(\kappa,R)$ and h(R) (Eq. 1) were given in a former paper (Ref. 2).

Volume fractions and size distributions were determined by least square fits of the theoretical cross sections to the measured $d\Sigma^{\perp}/d\Omega$. Finally, we determined the ratio:

$$B = \left(\frac{d\Sigma_{nuc}(\kappa)/d\Omega}{d\Sigma^{\perp}_{mag}(\kappa)/d\Omega}\right)^{1/2} \operatorname{sign}\left(\frac{\Delta\eta_{nuc}}{\Delta\eta_{mag}}\right) \qquad (2a)$$

where

Sign(x) = +1 for x > 0 and -1 for x < 0,

from the nuclear and magnetic scattering intensities. For nonferromagnetic clusters containing several elements i with concentrations $\nu_i (\sum_i \nu_i = 1)$, B is conveniently written as (Ref. 2):

$$B = \sum_i \frac{b_{nuc}^{matrix} - b_{nuc}^{i}}{b_{mag}^{matrix}} \nu_i = \sum_i s_i \nu_i \qquad (2b)$$

The slopes s_i are given by the coherent nuclear scattering length (b_{nuc}^{i}) of element i and the mean nuclear (b_{nuc}^{matrix}) and magnetic (b_{mag}^{matrix}) scattering lengths of the matrix, the latter being nearly equal to those of pure iron. Figure 1 which is based on Eq. 2b provides the basis for a determination of the cluster composition from SANS data.

2.3.1 Yield Strength Changes Due to Defect Structures

Russell and Brown proposed a dispersion hardening model (RB-model) for alloys containing precipitates or defects which are elastically softer than the surrounding matrix (Ref. 9). By means of this model they were able to describe the hardening due to Cu precipitates in Fe-Cu alloys quantitatively (Ref. 9). Later on, Fisher, et al., applied the RB-model to modelling the radiation hardening in Magnox pressure vessel steels (Ref. 10, 11).

In the framework of the RB-model, the increase in strength in alloys containing elastically soft precipitates is described by the following equations:

$$\tau = 0.8 \frac{Gb}{L} \left(1 - \left(\frac{E_1}{E_2}\right)^2\right)^{1/2} \quad \text{if } \arcsin \frac{E_1}{E_2} \leq 50^0 \qquad (3a)$$

$$\tau = \frac{Gb}{L} \left(1 - \left(\frac{E_1}{E_2}\right)^2\right)^{3/4} \quad \text{if } \arcsin \frac{E_1}{E_2} > 50^0 \qquad (3b)$$

where,

τ = shear stress

b = Burger's vector

L = Precipitate spacing in the slip plane

G = Shear modulus of the matrix.

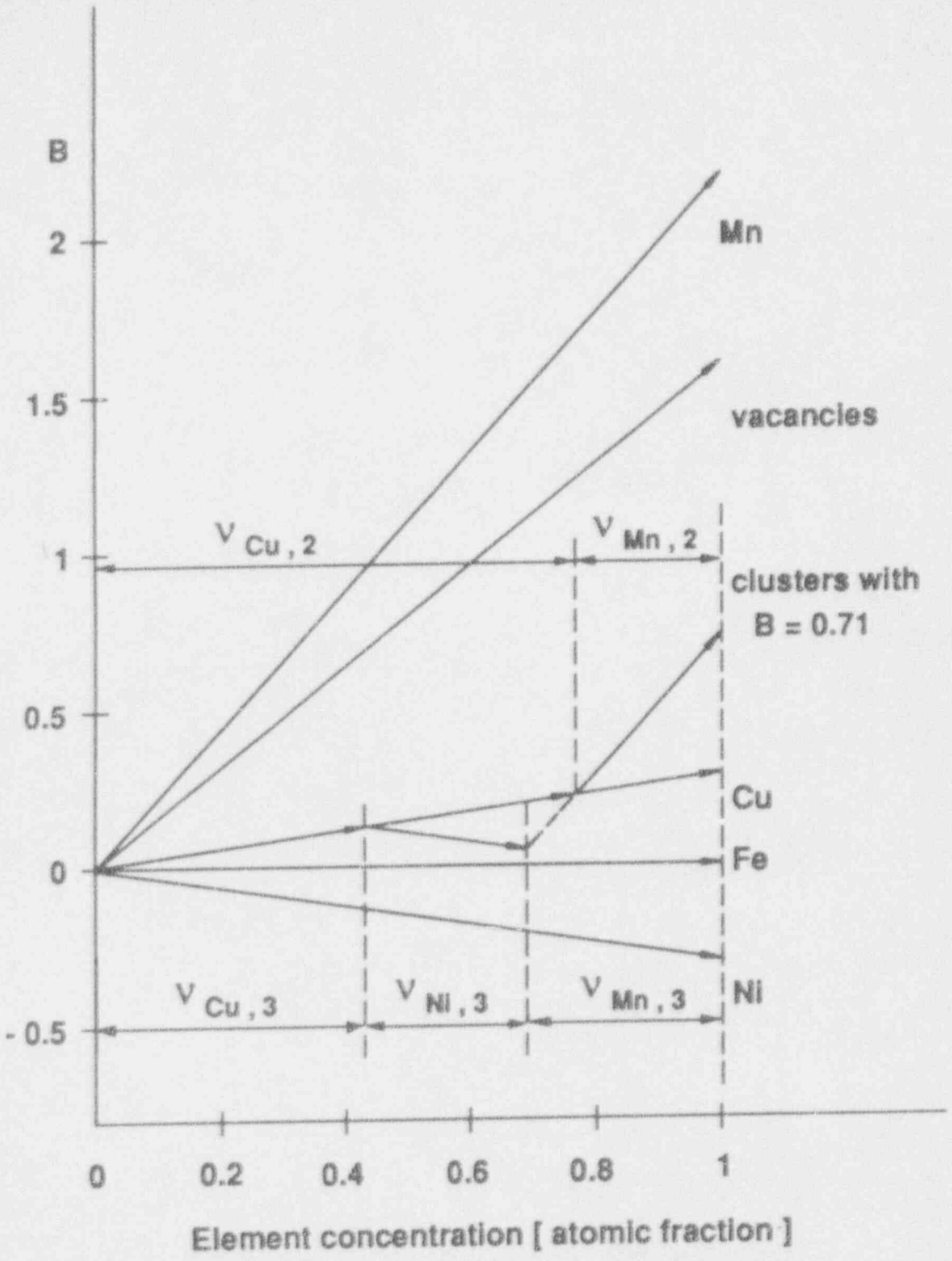

Fig. 1 Graphical representation of the determination of the ratio B for clusters containing different species i of atoms (i = Cu, Mn, Ni ...) according to Eq. 2b. A ratio of B = 0.71 can be obtained for a definite concentration $\nu_{Cu,2}$ and $\nu_{Mn,2}$ if the clusters are known to contain only these elements. If the clusters are composed of more than two elements, the corresponding concentrations cannot be determined unambiguously.

The ratio E_1/E_2 is determined by the energies per unit length E_1^∞ and E_2^∞ of dislocations in infinite media of the precipitated phase (Index 1) and the matrix phase (Index 2):

$$E_1/E_2 = e^\infty \frac{\log\frac{R}{r_o}}{\log\frac{r}{r_o}} + \frac{\log\frac{r}{R}}{\log\frac{r}{r_o}} \qquad (4)$$

where,

$r_o \approx 2.5b$

$R \approx 1000\ r_o$

$e^\infty = E_1^\infty/E_2^\infty$.

For calculating the yield strength from Eq. 3 and 4, Russell and Brown used a Schmid factor of 2.5.

In the framework of the RB-model, no hardening occurs if the shear moduli of the precipitate and the matrix phases are equal ($e^\infty = 1$). Maximum hardening is to be expected for voids ($e^\infty = 0$). For Cu precipitates in ferrite, Russell and Brown supposed $e^\infty = 0.6$. Assuming constant volume fractions, the RB-model predicts for Fe-Cu alloys maximum yield strengths if the precipitates have radii of $R \approx 1.25$ nm. This result is in good agreement with experimental results (Ref. 9).

3. RESULTS AND DISCUSSION

3.1 Defect Structures After Irradiation (I-condition)

3.1.1 Weld Deposits W8A, W9A, and WW7

During irradiation of W8A weld deposits to only 0.56×10^{19} n/cm^2, defects with diameters of ~ 1.6 nm and a volume fraction of ~ 0.21% were formed. Their size and volume fraction became almost twice as large upon irradiation to 3.85×10^{19} n/cm^2 (Table 3, Figs. 2 and 3). A ratio of B ~ 0.7 was measured which does not change with fluence. This value is typical for irradiated steels (Ref. 6, 7) and corresponds to Cu clusters containing ~ 20% at.% Mn. The Mn concentration would even be higher if elements such as Ni and Fe are also contained in the clusters (Fig. 1).

The I treatments of the weld deposits were performed with a fluence rate of ~ 9×10^{12} n/cm^2-s^{-1}; only for the irradiation of W8A to 3.85×10^{19} n/cm^2 was a much smaller fluence rate of ~ 0.7×10^{12} n/cm^2-s^{-1} applied. Figures 2 and 3 show that the evolution of the clusters is not significantly affected by the variation of the fluence rate although a minor effect cannot be excluded.

After irradiation to 1.44×10^{19} n/cm^2, the measured sizes, volume fractions, and B-ratios of the clusters in W9A and WW7 specimens differ very little from those in the W8A material. Thus, variations in the C and Si contents (W8A: C ~ 0.085 wt%, Si ~ 0.75 wt%; W9A: C ~ 0.19 wt%, Si ~ 0.23 wt%) or Ni contents (W8A: ~ 0.58 wt%; WW7: ~ 0.11 wt%) do not influence the cluster evolution significantly.

3.1.2 Low Alloy Steels 23F and 23G

The volume fractions and sizes of clusters formed in the 23F plate, irradiated with the highest fluence rate (9×10^{12} n/cm^2-s^{-1}) to a fluence of ~ 0.5×10^{19} n/cm^2 are much smaller than those generated in the W8A weld deposit subjected to the same irradiation (Table 3). At first glance, this seems to correlate with the lower Cu and Ni contents of the 23F material compared with the W8A weld deposit. During further irradiation, however, the defects in the 23F plate grow significantly faster than those in the W8A weld. After a fluence of 2.23×10^{19} n/cm^2, the defect volume fractions are nearly equal in both materials and the cluster sizes in the 23F plate (D ~ 3 nm) are even larger than those in W8A weld deposits (D ~ 2.2 nm). Thus, we conclude that apart from composition, a further--still unknown--factor strongly influences the defect growth kinetics.

Defects formed in the 23G plate during irradiation to 0.49×10^{19} n/cm^2 with the high fluence rate have comparable volume fractions and sizes but significantly larger B ratios than those in the 23F plate (Table 3). With respect to the higher Ni content of the 23G plate, the larger B ratio is surprising since B would rather decrease if clusters were only enriched with Ni. B would increase, however, if the clusters were not only enriched with Ni but also with Mn.

Table 3 Number Densities, Mean Diameters, Width Parameters, Volume Fractions, and B Ratios of Defects in Welds and Plates from Commercial Production

Sample	I Condition		Number[c] Density	Mean Diameter	Width Parameter	Volume Fraction	Ratio[d]
	Fluence[a]	Fluence Rate[b]					
	F	$\dot{F}$	N_v	D	p	f	B
				(nm)		(%)	
W8A-372	0.56	9	8.9	1.6	0.21	0.21	0.73
W8A-518	1.44	9	5.7	2.1	0.23	0.27	0.67
W8A-351	2.23	9	5.2	2.2	0.25	0.30	0.71
W8A-266	3.85	0.7	3.5	2.7	0.24	0.35	0.73
W9A-412	1.44	9	4.9	2.2	0.27	0.30	0.71
WW7-63	1.44	9	4.0	2.2	0.36	0.24	0.67
23F-68	0.56	9	---	1.2	0.25	0.10	0.61
23F-108	0.54	0.08	1.7	2.4	0.24	0.12	0.59
23F-67	2.23	9	2.0	3.0	0.29	0.28	0.59
23F-4	3.85	0.7	1.9	2.4	0.26	0.14	0.75
23G-212	0.45	9	---	1.2	0.25	0.10	0.91
23G-183	0.54	0.08	3.6	2.2	0.28	0.15	0.79

[a] $F \times 10^{19}$ n/cm^2 [b] $\dot{F} \times 10^{12}$ n/cm^2-s^{-1} [c] $N_v \times 10^{17}$ cm^{-3}

[d] Ratio B of defects in irradiated samples

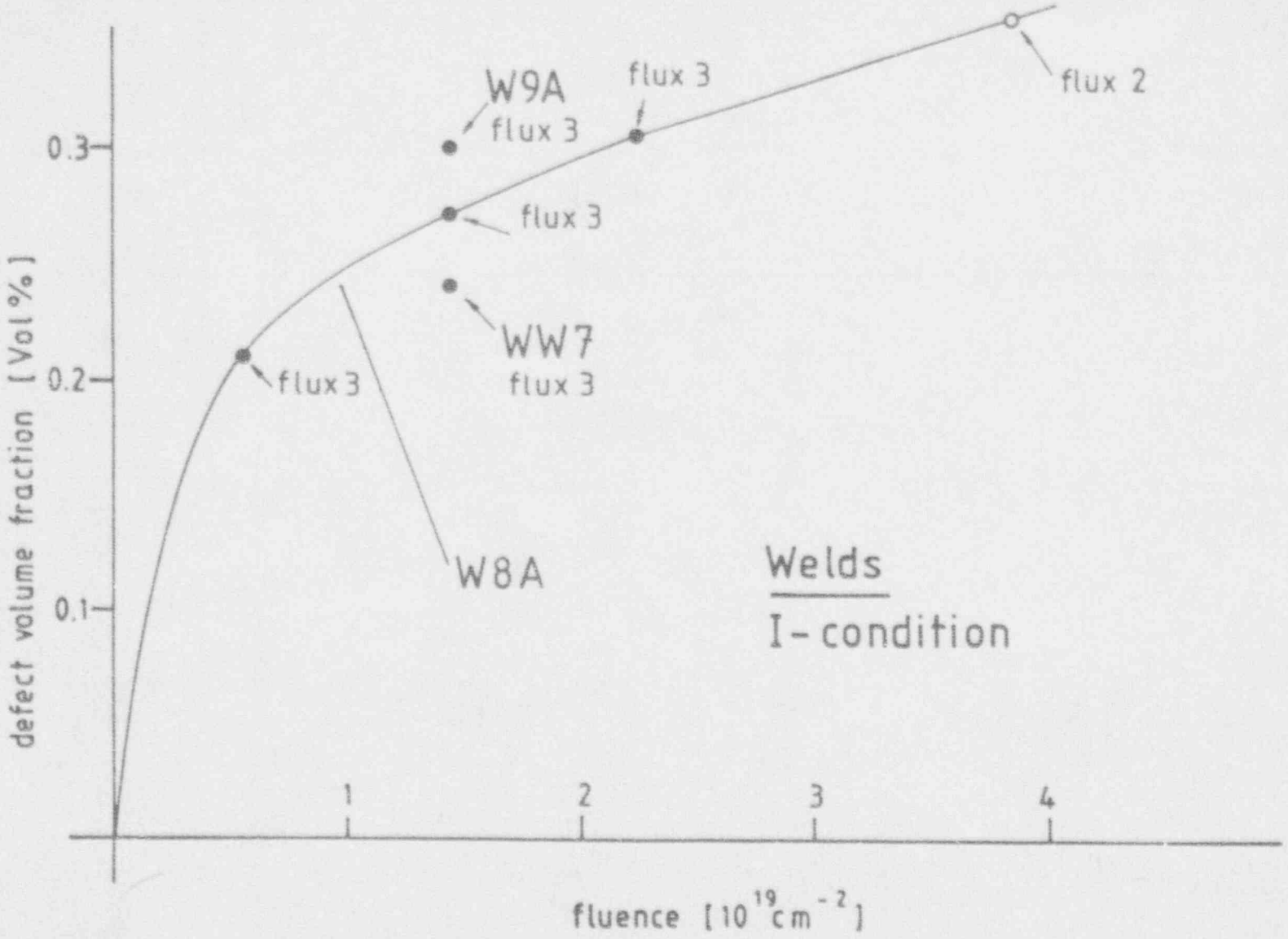

Fig. 2 Defect volume fractions in the weld deposits after irradiation as a function of the fast neutron (E > 1 MeV) fluence. Fluence rates, in units of 10^{12} n/cm^2-s^{-1}, are: flux-1 = 0.08, flux-2 = 0.7, and flux-3 = 9.0.

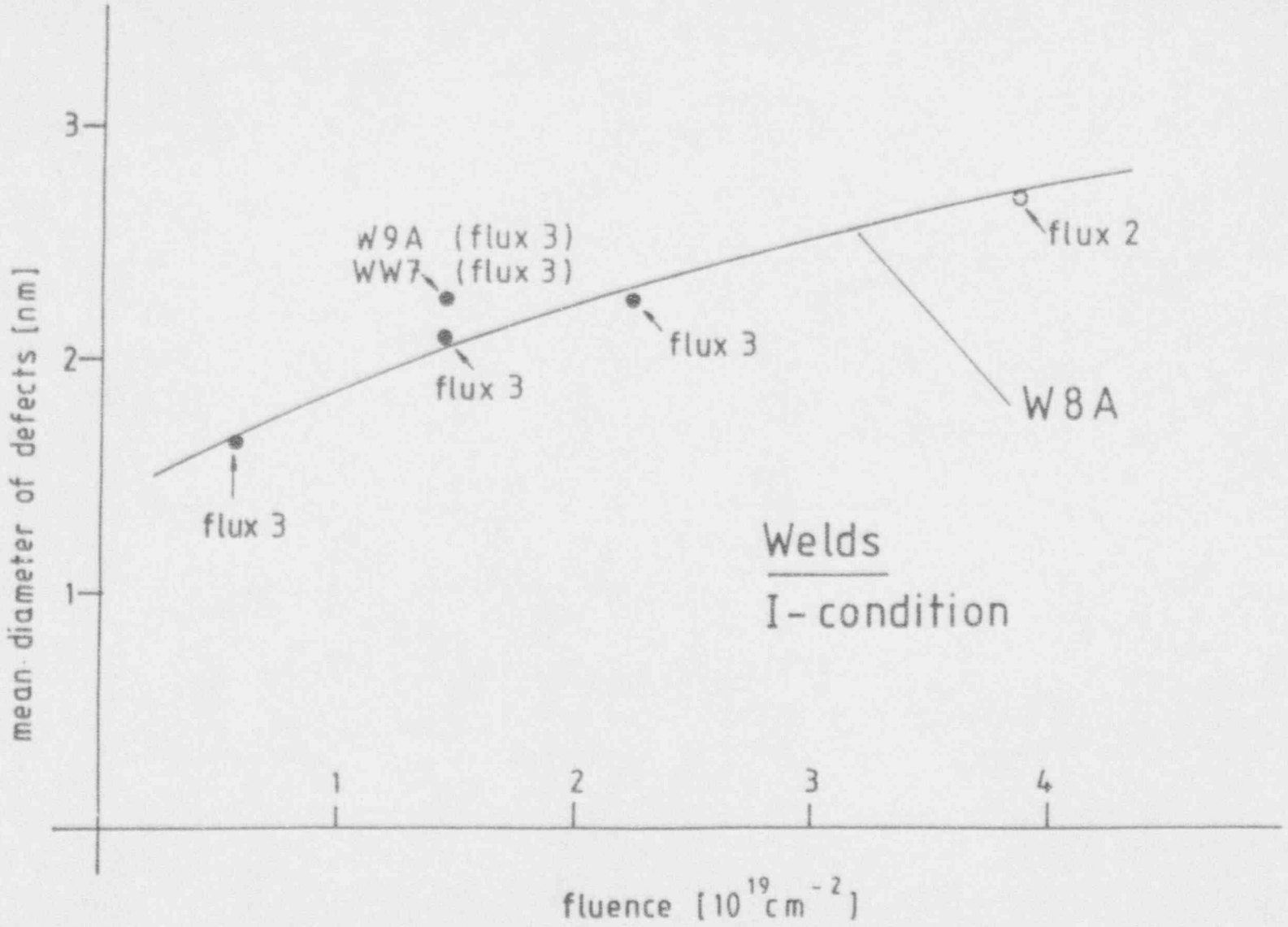

Fig. 3 Mean diameters of the clusters in the weld deposits after irradiation as a function of the fast neutron (E > 1 MeV) fluence. Fluence rates, in units of 10^{12} n/cm^2-s^{-1}, are: flux-1 = 0.08, flux-2 = 0.7, and flux-3 = 9.0.

In contrast to the weld deposits, a clear fluence rate dependence of the defect forming and growth mechanism could be observed for the 23F and 23G plates. Irradiation to ~ 0.55 x 10^{19} n/cm^2 with either a high or a low fluence rate (9.0 or 0.8 x 10^{12} n/cm^2-s^{-1}) yields in both cases nearly identical defect volume fractions and B ratios. Under the low fluence rate irradiation, the defect diameters become twice as large with respect to the high rate irradiations (Figs. 4 and 5, Table 3). The opposite fluence rate dependence has been observed for higher fluences. Irradiation of the 23F plate to 3.85 x 10^{19} n/cm^2 with an intermediate rate (0.7 x 10^{12} n/cm^2-s^{-1}) leads to cluster diameters of 2.3 nm whereas during irradiation to only 2.23 x 10^{19} n/cm^2 with a high rate (9.0 x 10^{12} n/cm^2-s^{-1}), clusters with mean diameters of 3.0 nm are formed (Table 3). These observations, especially the apparently contradicting fluence rate effects of low vs. high fluences, suggest rather complicated defect growth kinetics and are not yet understood.

3.2 Defect Structures in Irradiated and Annealed Laboratory-Melted Plates

During irradiation of the 67C plate from a laboratory melt (Cu content ~ 0.002 wt%) to a fluence of 2.5 x 10^{19} n/cm^2, void-like defects with a total volume fraction of ~ 0.05% and diameters of ~ 1.2 nm are formed (Ref. 2 and Table 4). After annealing this material for 168 h at 399°C, the volume fraction and the diameters of the defects decreased to 0.01% and 0.9 nm, respectively. Furthermore, the scattering data show the B ratio to increase during this annealing from ~ 0.8 to ~ 1.6, the latter being characteristic for voids. Two conclusions can be drawn from these observations. First, likely solute segregation at the surface of the voids dissolves at 399°C leaving behind pure voids (Ref. 2). Second, the precipitated clusters are thermodynamically unstable at 399°C and are expected to disappear completely after extended annealing.

Irradiation of the 68A plate material (0.30 wt% Cu) to a fluence of 2.5 x 10^{19} n/cm^2 leads to defects with diameters of ~ 2.3 nm, a volume fraction of ~ 0.4%, and a B ratio of ~ 0.67 (Ref. 2, Table 4, and Fig. 6). These clusters nearly double their size, decrease their B ratio to a value of ~ 0.46, and nearly halve their volume fraction during annealing for 168 h at 454°C. This indicates that during this thermal treatment these defects (a) become enriched with Cu and (b) are stable because they are able to grow (Ref. 2). During annealing this material at the lower temperature of 399°C, the defects show only little growth and their volume fraction is decreased only by half the amount found with the 454°C anneal. Furthermore, during annealing at 399°C, the B value decreases only to ~ 0.6. From this result, we conclude that the defects are also stable at 399°C. The thermodynamic forces governing the composition changes, however, seem to be very different at the two annealing temperatures under consideration. This is especially concluded from the different B values found after the different annealing treatments as the compositional changes within the defects are expected to occur much faster at a given aging temperature than significant changes of their sizes or volume fractions.

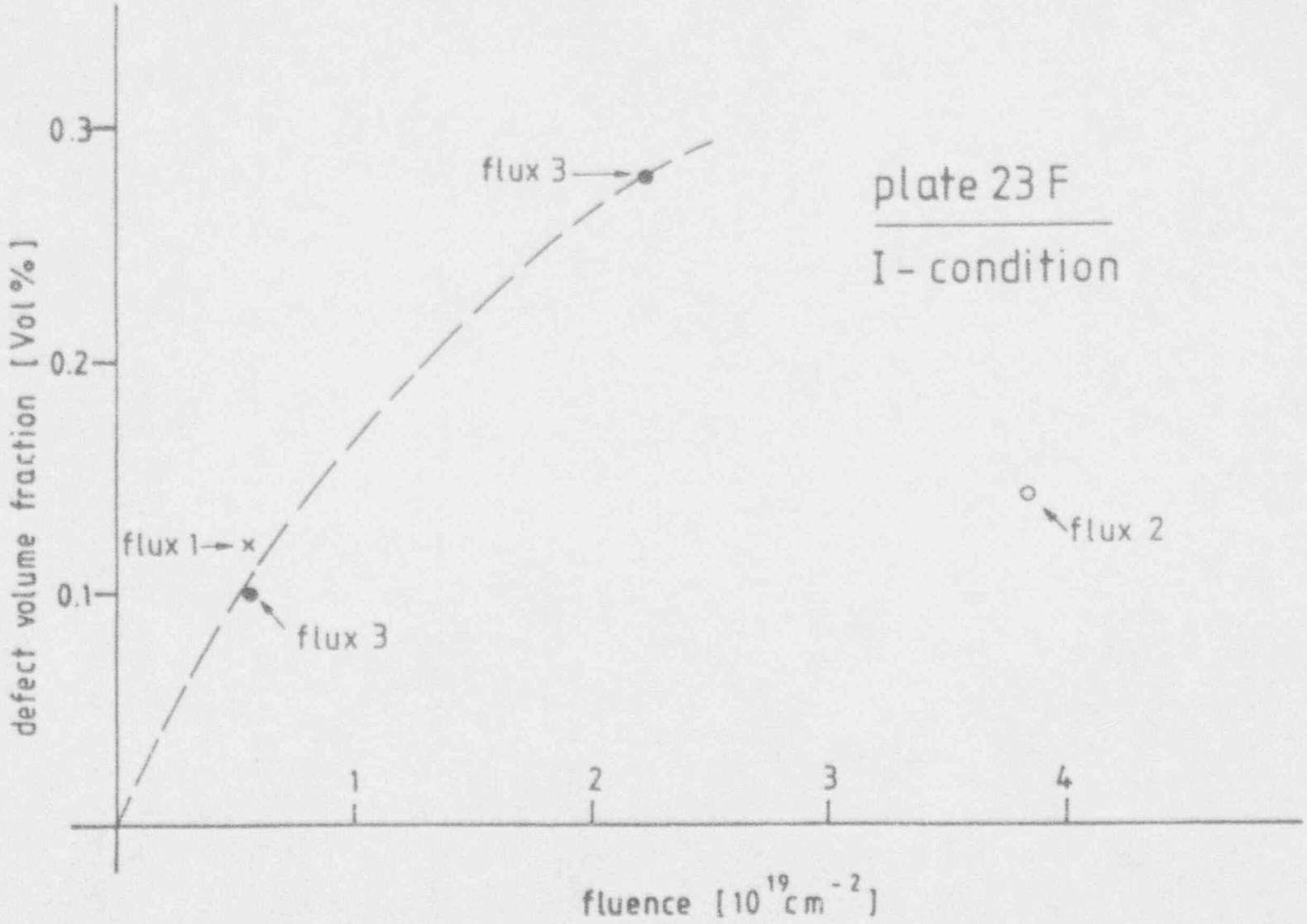

Fig. 4 Defect volume fractions in Plate 23F from a commercial melt as a function of the fast neutron (E > 1 MeV) fluence. Fluence rates, in units of 10^{12} n/cm^2-s^{-1}, are: flux-1 = 0.08, flux-2 = 0.7, and flux-3 = 9.0.

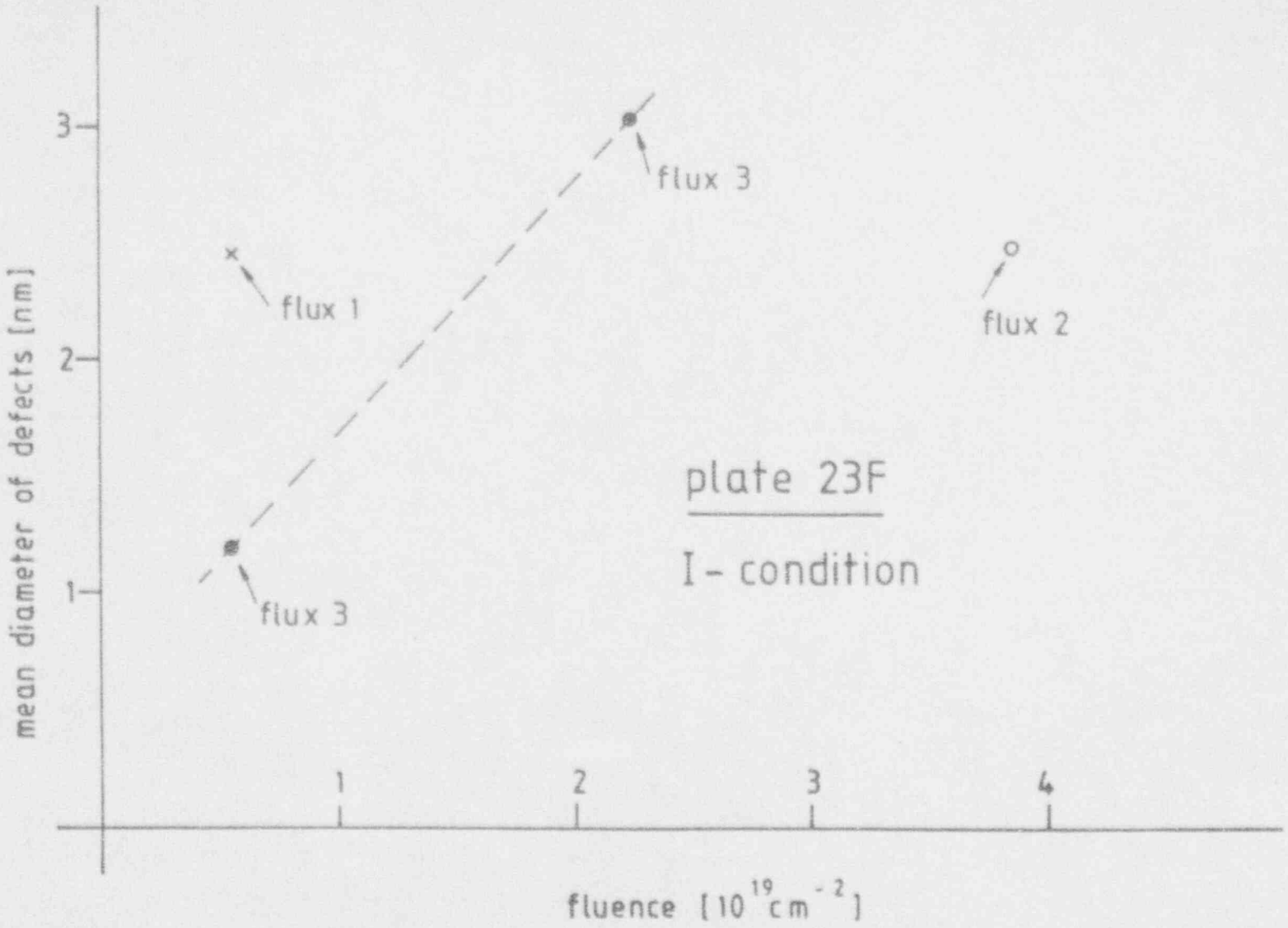

Fig. 5 Mean diameters of the clusters in Plate 23F from a commercial melt as a function of the fast neutron (E > 1 MeV) fluence. Fluence rates, in units of 10^{12} n/cm^2-s^{-1}, are: flux-1 = 0.08, flux-2 = 0.7, and flux-3 = 9.0.

Table 4 Number Densities, Mean Diameters, Width Parameters, Volume Fractions, and B Ratios of Defects in Laboratory Melts

Sample	Sample[a] Condition	Anneal[b] Temp T_A (°C)	Number[c] Density N_v	Mean Diameter D (nm)	Width Parameter p	Volume Fraction f (%)	Ratio[d] B
68A-10	I-7[e]	---	6.6	2.3	0.19	0.40	0.67
68A-10	IA-1	399	3.5	2.5	0.34	0.27	0.60
68A-12	IA-2[e]	454	0.3	4.9	0.39	0.18	0.46
68C-32	I-7[e]	---	26	1.5	0.27	0.46	0.67
68C-32	IA-1	399	4.2	2.2	0.33	0.23	0.59
68C-38	IA-2[e]	454	0.25	5.0	0.34	0.16	0.49
67C-4	I-7[e]	---	---	1.2	0.25	0.05	0.85
67C-4	IA-1	399	---	0.9	0.40	0.01	1.60

[a] Fluence 2.5×10^{19} n/cm^2; I-7 = after irradiation; IA-1, IA-2 = after irradiation and annealing

[b] Annealing time = 168 h (see also Table 2)

[c] $N_v \times 10^{17}$ cm^{-3}

[d] Ratio B of defects in laboratory melts after irradiation or after irradiation and annealing

[e] Previous investigation (Ref. 2)

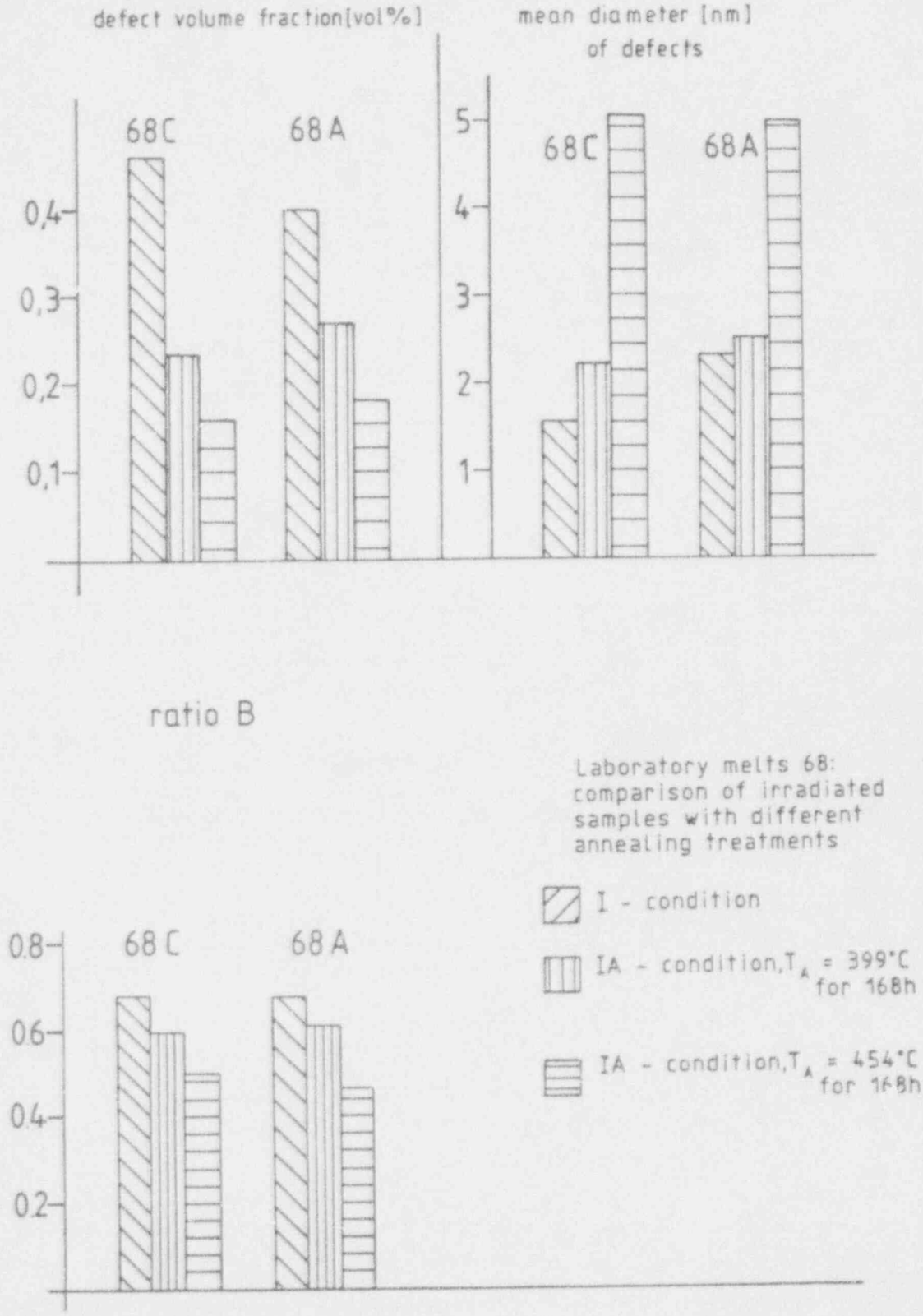

Fig. 6 Defect structures in Plates 68C and 68B from laboratory melts after irradiation and annealing treatments.

3.3 Development of Defects in Weld Deposits During Reirradiation

Scattering curves of reirradiated weld deposits have been found to deviate significantly from those of only irradiated or irradiated and annealed samples. The latter ones show a steep slope in the range of large scattering vectors. This is a general feature of SANS intensities resulting from simple-structured clusters with a single peaked size distribution. The scattering intensity in this region of large scattering vectors depends mainly on the total surface of all clusters and changes to a κ^{-4} dependence for even larger vectors (Fig. 7a). Scattering curves for the weld deposits in the IAR condition show, however, additional scattering contributions at large κ (Figs. 7b and 7c). These can be interpreted as a superposition of SANS intensities from clusters having two considerably different mean sizes (bimodal size distribution).

In the case of the 454°C annealed samples, the two scattering contributions can clearly be separated from each other, because they appear in sufficiently separated scattering vector regions. This definitely indicates a difference in the sizes of the two kinds of defects (Fig. 7c). However, the overlap of the two scattering contributions prevents the two mean sizes and volume fractions from being determined as precisely as in the case of singly peaked cluster distributions (Table 5). In the case of 399°C annealed samples, the scattering contribution of the small clusters is heavily covered up by that of the large ones (Fig. 7b) This leads to rather large uncertainties with respect to the characterization of the small defects (Table 5). [It should be mentioned that bimodal size distributions in preannealed and irradiated as well as in annealed and reirradiated materials have already been reported in previous papers (Refs. 2, 6, 7, 12, 13).]

The large clusters (also referred to as 1st-size distribution or indexed with "1") in 454°C annealed IAR samples show nearly no change in their diameters, volume fractions, and B ratios between reirradiation fluences of 0.37 and 1.12×10^{19} n/cm^2 (Table 5, Fig. 8). Compared to those defects found in the corresponding, though only irradiated materials (see Sec. 3.1), the large clusters in IAR samples are about three times larger, their volume fractions are significantly smaller (WW7 ~ 20%; W8A and W9A ~ 50%), and their B ratios are only ~ 0.47 instead of ~ 0.68 as in the I condition. Furthermore, the 1st size distributions yield similar diameters, volume fractions, and B ratios as those found in the 68A and 68C laboratory melts after 454°C annealing (Table 4).

The large clusters observed in the 399°C annealed and reirradiated weld deposits W8A and WW7 correspond rather well to those found in the 68A and 68C plates after annealing at this temperature (Tables 5 and 4). The large defects found in WW7 weld deposits are rather stable during reirradiation; no changes in their size, B ratio, or volume fraction were observed with increasing reirradiation fluence.

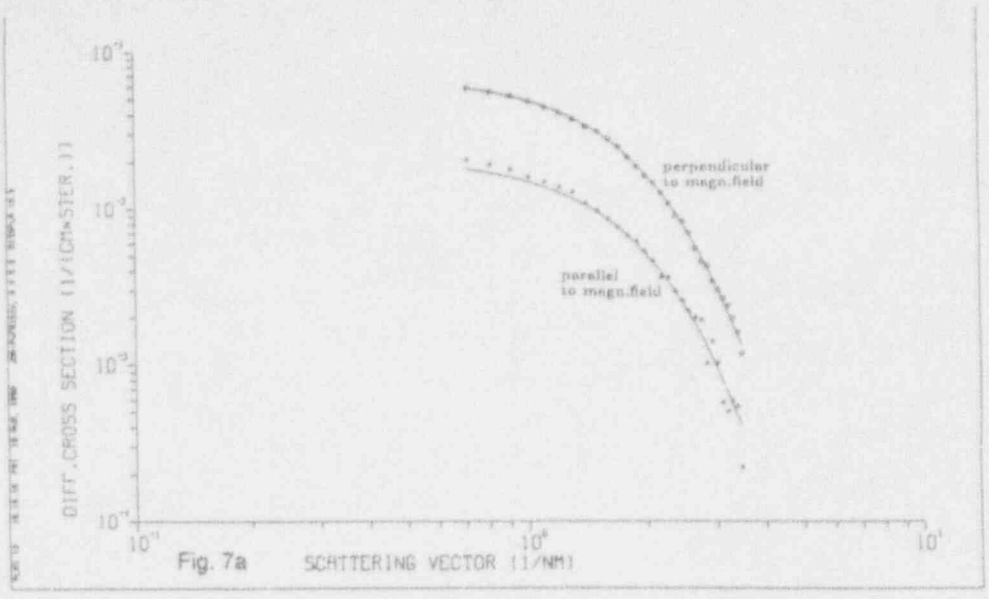

Fig. 7a

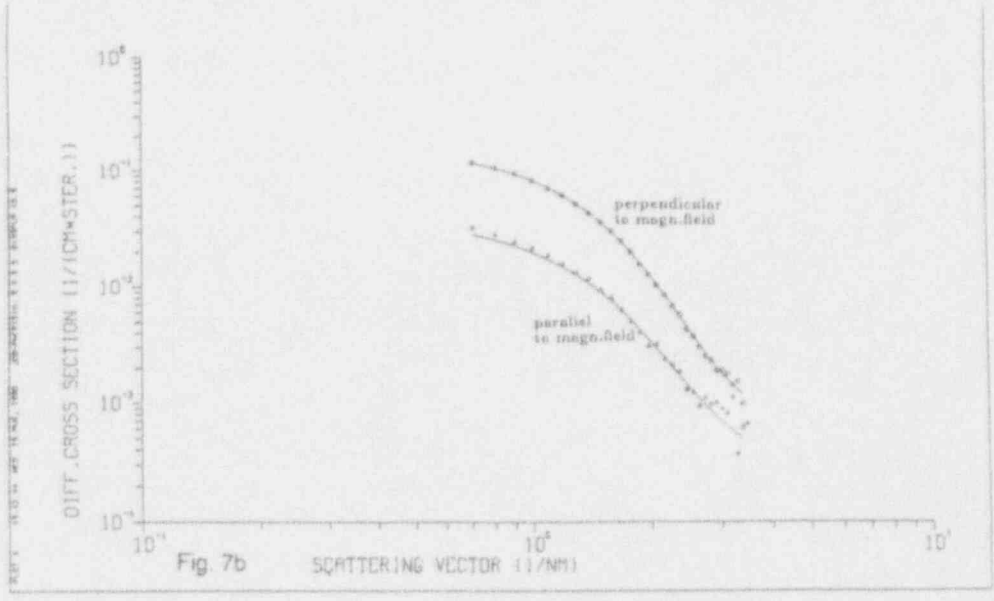

Fig. 7b

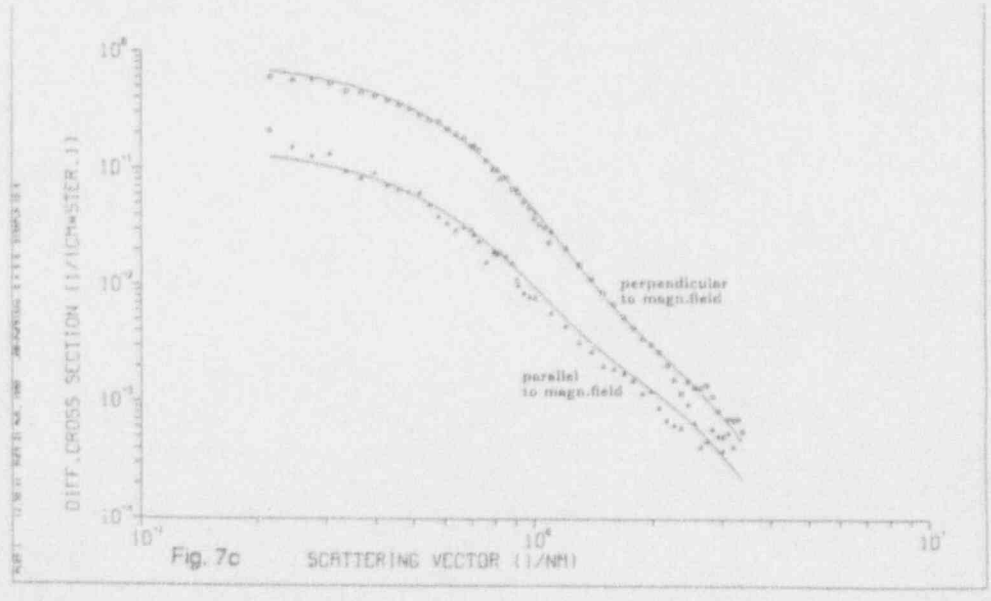

Fig. 7c

Fig. 7 SANS intensities measured parallel and perpendicular to the sample magnetization for weld deposit W8A after I-4 irradiation (Fig. 7a), after IAR-2 reirradiation (Fig. 7b), and IAR-4 reirradiation (Fig. 7c).

Table 5 Defect Sizes, Volume Fractions, and B Ratios of Weld Deposits After I[a] and IAR Treatments

Sample	Sample Condition	Fluence 2[b]	Annealing Temp T_A (°C)	Mean[c] Diameter D_1 (nm)	Volume Fraction f_1 (%)	Ratio B_1	Mean[d] Diameter D_2 (nm)	Volume Fraction f_2 (%)	Ratio B_2
WW7-6	I-4	----	---	2.2	0.24	0.67	---	-----	---
WW7-66	IAR-1	0.37	399	3.6	0.21	0.46	1.7±0.3	0.014±0.004	1.6
WW7-95	IAR-2	1.09	399	3.4	0.21	0.50	1.2±0.4	0.023±0.004	1.6
WW7-24	IAR-3	0.37	454	6.2	0.18	0.47	2.3±0.3	0.008±0.003	1.6
WW7-106	IAR-4	1.12	454	6.0	0.20	0.47	1.5±0.3	0.011±0.002	1.6
W9A-412	I-4	----	---	2.2	0.30	0.71	---	-----	---
W9A-362	IAR-1	0.37	399	3.1	0.26	0.58	1.0±0.4[e]	0.011±0.005	1.6
W9A-427	IAR-4	1.12	454	5.3	0.16±0.03	0.47	1.4±0.3	0.011±0.002	1.6
W8A-518	I-4	----	---	2.1	0.27	0.67	---	-----	---
W8A-160	IAR-1	0.37	399	2.3	0.29	0.62	---	-----	---
W8A-472	IAR-2	1.09	399	2.8	0.27	0.55	1.0±0.4[e]	0.016±0.005	1.6
W8A-446	IAR-3	0.37	454	5.9	0.18	0.48	1.5±0.3	0.005±0.001	1.6
W8A-486	IAR-4	1.12	454	5.9±0.9	0.14±0.004	0.43	1.6±0.4	0.013±0.004	1.6

[a] Fluence 1 = 1.44 x 10^{19} n/cm^2; annealing time = 168 h [b] x 10^{19} n/cm^2

[c] Index 1 refers to the size distribution formed mainly during the I and IA treatments.

[d] Index 2 refers to a second (smaller) size distribution of defects formed during the reirradiation treatment, except for sample W8A160, where it could not be detected.

[e] Estimated values

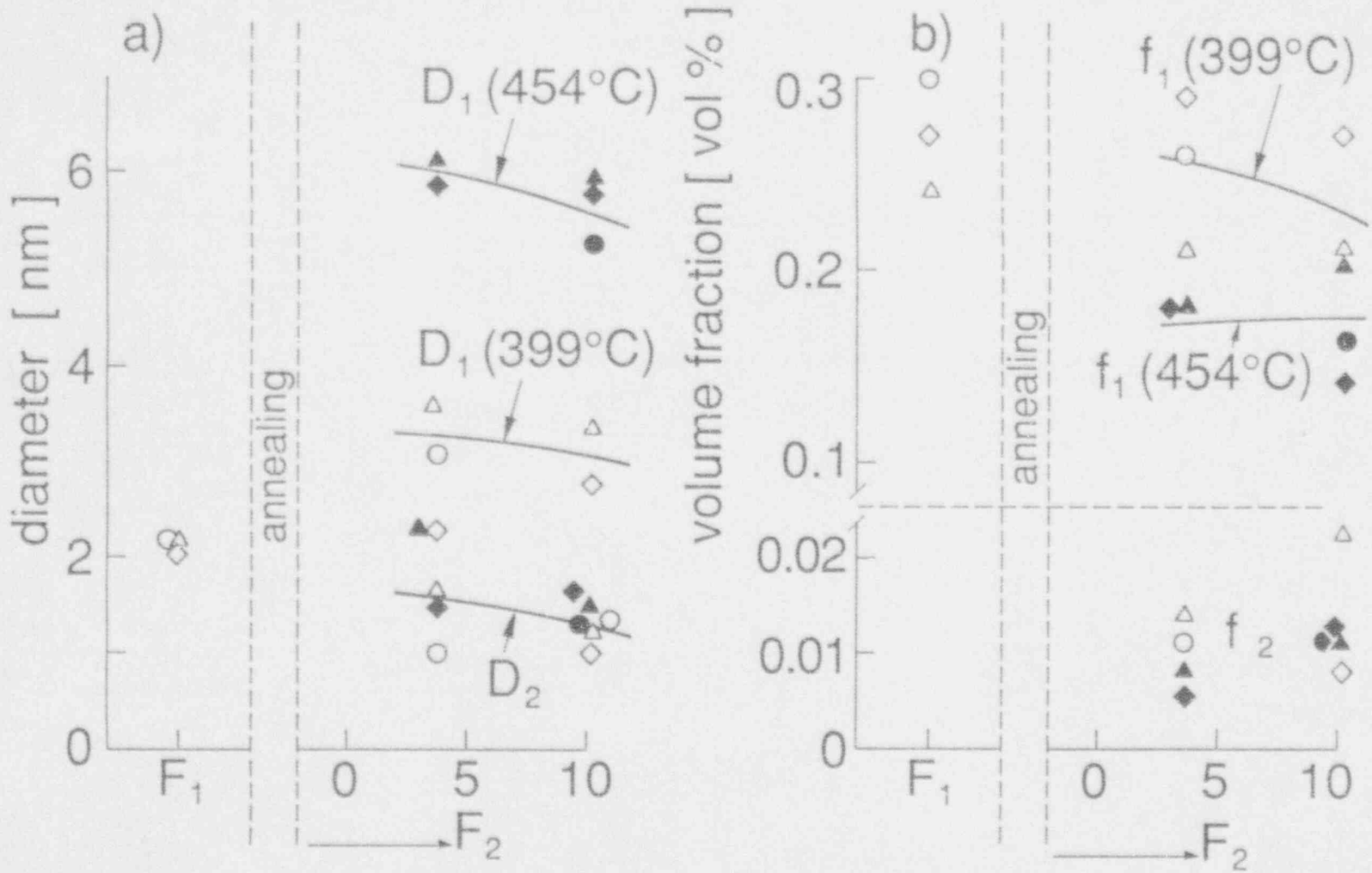

Fig. 8 Diameters and volume fractions of defects in weld deposits WW7 (▽ and ▼), W9A (○ and ●), and W8A (◇ and ◆) in the I condition (fluence F_1 = 1.44 x 10^{19} n/cm^2) and in the IAR condition (F_2 reirradiation fluence). Open and filled symbols refer to samples annealed at 399°C and 454°C, respectively.

The defect structure of the weld deposits after annealing will be analyzed in a forthcoming paper. On the basis of the present results we can assume, however, that the stable clusters found after the reirradiations were already formed during the preceding annealing treatments. This means that solute atoms which are precipitated in these large clusters will not be redissolved and will, thus, have little influence on the formation of the small defects (2nd-size distribution) during reirradiation. Thus, we expect these defects in the weld deposits to be comparable with those which have been found in materials with rather low contents of Cu and Ni. This expectation has indeed been justified by the features of the small clusters (2nd-size distribution in Table 5; Fig. 8). Their sizes and B ratios do not differ much from those of the defects found in irradiated 67C laboratory melts which are nearly free of Cu (Tables 4 and 1). The volume fractions of the small clusters in the reirradiated weld deposits are even lower than those of the defects in the irradiated 67C melt.

3.4 Radiation Hardening and Defect Structure

The shift of the transition temperature caused by the various I, IA, and IAR treatments of the materials is closely related to the corresponding changes of the yield strength (Fig. 9). In the following we have attempted to interpret the measured tensile properties of the various materials in terms of the RB-model (Eqs. 3, 4) by using the relevant parameters of the defect microstructure which were derived from SANS.

The defects in the Cu-containing materials were found to be Cu-rich precipitates after the I treatments (Table 3 and Sect. 3.1). We calculated their hardening contribution according to Eq. 3 and 4 on the basis of their volume fractions and radii assuming a ratio $e^{\infty} = 0.6$ which corresponds to that of pure Cu precipitates. We found a surprisingly good agreement between the calculated and the measured yield strength changes (Fig. 10a). Thus, we concluded (a) the defects analyzed by SANS to be the reasons for the observed irradiation hardening and (b) the defects in the irradiated-only materials to be elastically nearly as soft as pure copper.

After reirradiation of the materials, large precipitates and small void-like defects were identified by SANS (see Table 5 and Sect. 3.3). First, we calculated their hardening contributions assuming a ratio of $e_p^{\infty} = 0.6$ for the precipitates and $e_v^{\infty} = 0$ for the voids. The total yield strength changes were determined according to $\Delta\sigma = \left(\Delta\sigma_p^{\,2} + \Delta\sigma_v^{\,2}\right)^{1/2}$. These calculated values, however, do not agree with the measured ones (Fig. 10b). The largest deviations were found for materials annealed at 454°C; the calculated yield strength changes exceed the measured values by a factor of ~ 2.5. The observed hardening in these alloys, however, appears to be to be caused solely by the hardening contribution $\Delta\sigma_v$ of the void-like defects ($\Delta\sigma_p = 0$). From this we conclude that during the 454°C annealing, the large defects lost most of their hardening efficiency. On grounds of the RB-model, this means that during this annealing the shear modulus

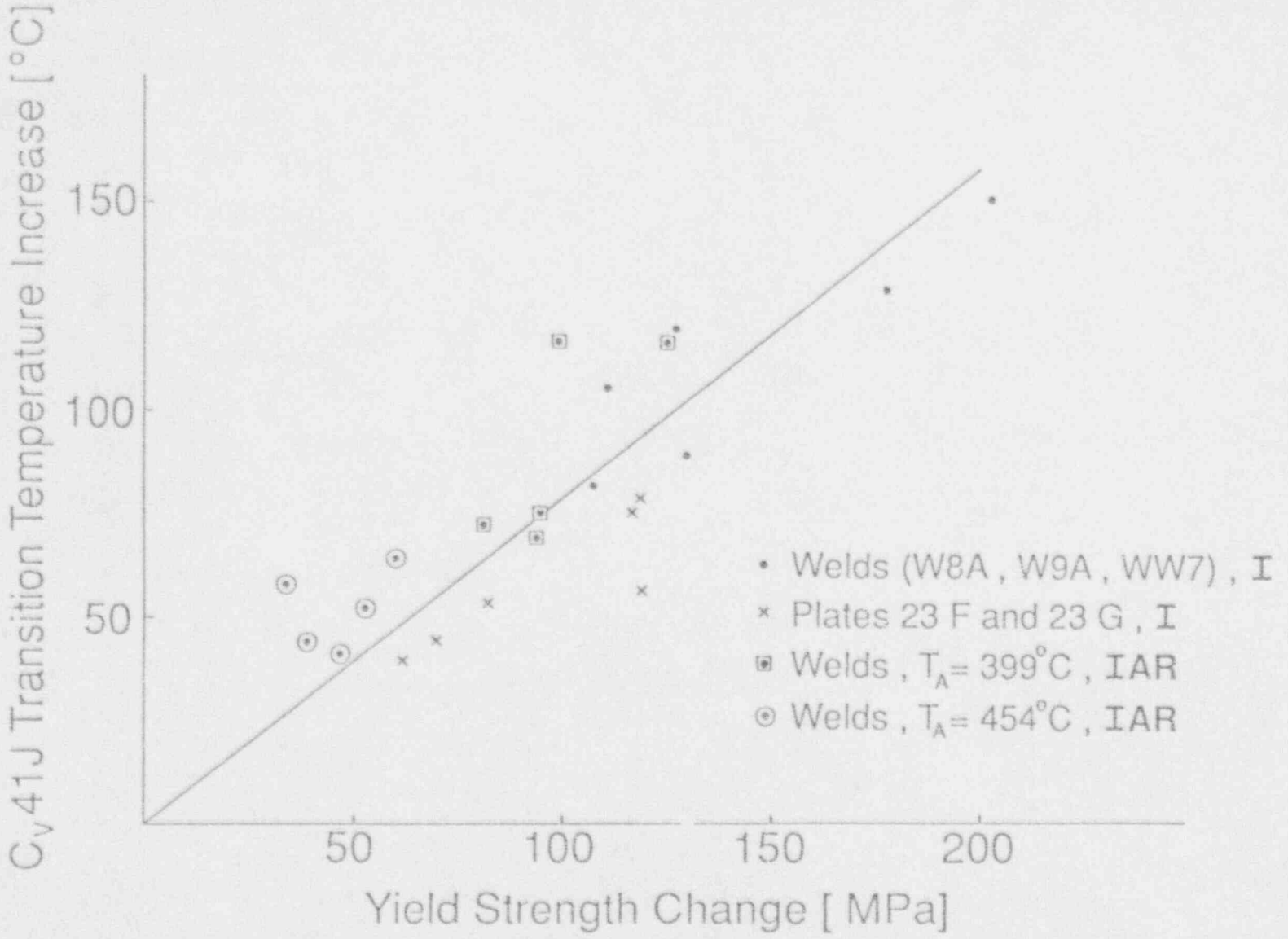

Fig. 9 Correlation of the increase in transition temperature vs. the increase in yield strength.

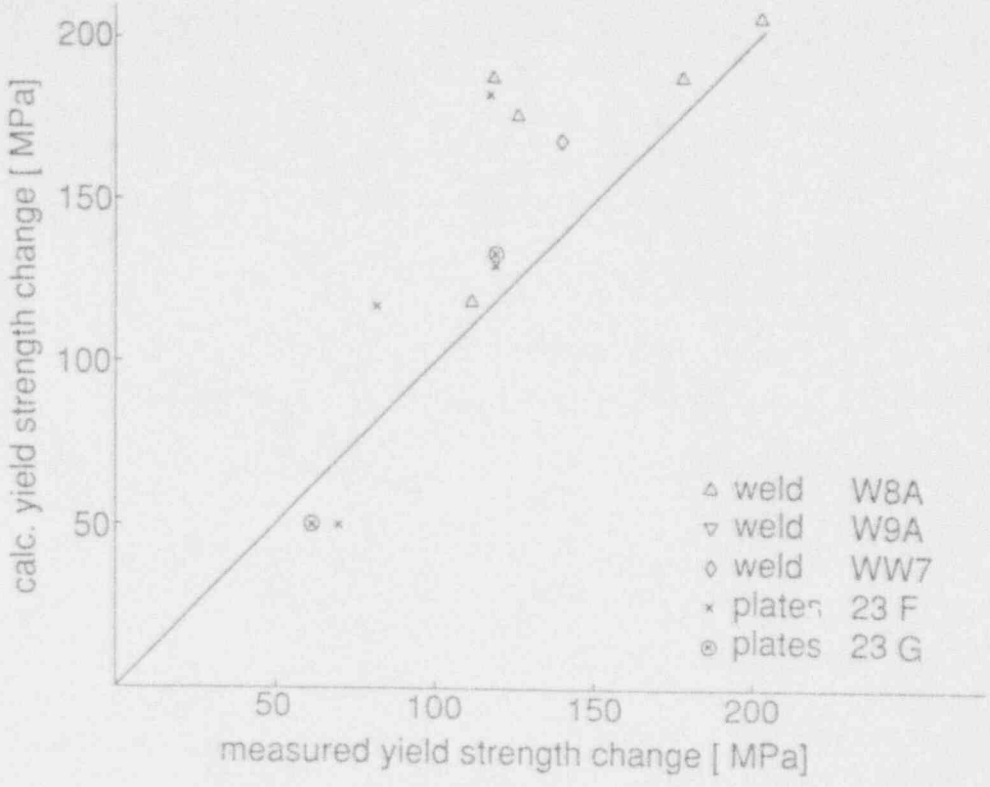

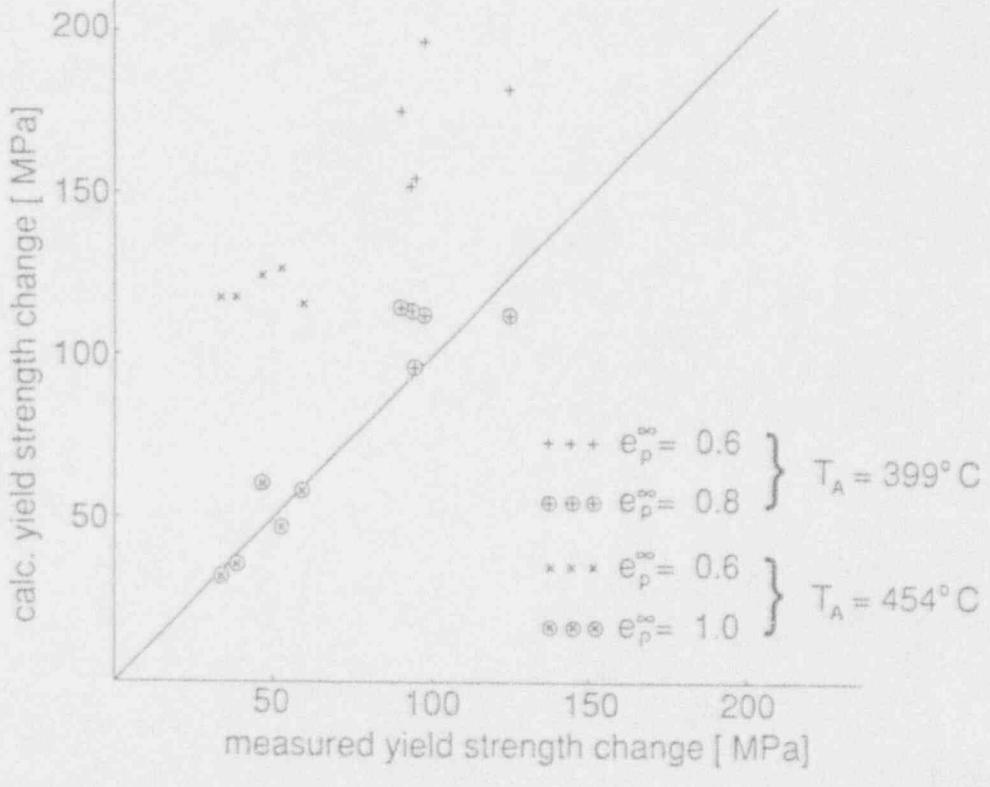

Fig. 10 Comparison of the measured yield strength changes with those calculated in the framework of the RB-model on the basis of the SANS data. The upper graph is the comparison for materials in the I condition; $e_p^\infty = 0.6$ (Eq. 4) is assumed. The lower graph is the comparison for weld deposits WW7, W9A, and W8A in the IAR condition.

of the large defects was increased by a factor of ~ 1.6 to a value nearly equal to that of the surrounding matrix. This interpretation is supported by the SANS analysis which shows a decrease of the B ratio from values of ~ 0.68 after irradiation to only ~ 0.48 after postirradiation annealing (Table 5). This reflects a considerable change in the chemical composition.

In the case of 399°C annealed materials, a rather good correspondence of calculated and measured yield strength changes is obtained if a ratio $e_D^{\infty} = 0.8$ is assumed for the large Cu-containing precipitates (Fig. 10b). This reflects an increase of the shear modulus of the precipitates during this annealing to a value which lies between the one found directly after irradiation and the one found after the 454°C anneal. This agrees with the findings concerning the change of the B value during the two annealing treatments.

4. SUMMARY AND CONCLUSIONS

Cu-rich clusters formed in the W8A, W9A, and WW7 weld deposits during irradiation are rather similar with respect to their sizes, B ratios, and volume fractions. Their B ratios, and thus their compositions, do not appear to be dependent on the applied fluence whereas their sizes and volume fractions grow significantly with progressing irradiation.

In contrast to the weld deposits, a clear fluence rate dependence (see Sect. 3.1.2) of the cluster forming kinetics has been observed in the 23F and 23G plates from commercial production melts.

Void-like defects in the 67C plate from a laboratory melt (very low Cu content) are unstable with respect to annealing at 399°C because their sizes and volume fractions are reduced during this treatment. In contrast, Cu-rich clusters in the 68A and 68C plate samples have been found to be stable during annealing at 399°C as well as at 454°C. Their sizes and B values, however, are increased and their volume fractions are decreased by this aging procedure. Furthermore, these changes in the defect structures are strongly temperature dependent.

The weld deposits W8A, W9A, and WW7 have not been analyzed in the IA condition. After reirradiation they contain large, Cu-rich clusters, as well as small, void-like defects. The large clusters correspond with respect to their sizes, B ratios, and volume fractions to those found in the 68A or 68C plate materials after annealing at 399°C or 454°C, respectively. Only small changes of their sizes, volume fractions, and B ratios were observed during reirradiation. Thus, the large clusters are rather stable during reirradiation and bind a large part of the Cu dissolved originally in the matrix. This result finally explains the results that the small clusters in reirradiated weld deposits are--with respect to their sizes, volume fractions, and B ratios--rather similar to those which are formed during irradiation of Cu-free steels such as the 67C plate from a laboratory melt.

A strong correlation was found between the shift of the transition temperature and the yield strength change. The latter could be explained on the basis of the defect microstructure determined by SANS analysis and the dispersion strengthening model of Russell and Brown. After annealing treatments, the hardening efficiency of the precipitates is significantly less than in the irradiated condition. From this it is concluded that the shear modulus of the precipitates increases during the annealing treatment.

REFERENCES

1. Proceedings of the 2nd International Symposium on Environmental Degradation of Materials in Nuclear Power Systems-Water Reactors, American Nuclear Society, LaGrange Park, IL, 1986.

2. P. A. Beaven, F. Frisius, R. Kampmann, R. Wagner, and J. R. Hawthorne, "SANS Investigation of Irradiated A 533-B Steels Doped with Phosphorus," in Radiation Embrittlement of Nuclear Reactor Pressure Vessel Steels: An International Review, L. E. Steele, Ed., ASTM STP 1011, Vol. 3, American Society for Testing and Materials, Philadelphia, PA, 1989, p. 243.

3. P. A. Beaven, F. Frisius, R. Kampmann, and R. Wagner, "Atomic Transport and Defects in Metals by Neutron Scattering," in Springer Proceedings in Physics 10, C. Janot, W. Petry, D. Richter, and T. Springer, Eds., Springer-Verlag, Berlin, Germany, 1986, p. 228.

4. S. P. Grant, S. L. Earp, S. S. Brenner, M. G. Burke, "Phenomenological Modeling of Radiation Embrittlement in Light Water Reactor Vessels with Atom Probe and Statistical Analysis," in Proceedings of the 2nd International Symposium on Environmental Degradation of Materials in Nuclear Power Systems-Water Reactors, American Nuclear Society, LaGrange Park, IL, 1986, p. 385.

5. F. Frisius and D. Bunemann, "The Measurement of Radiation Defects in Iron Alloys by Means of Small Angle Neutron Scattering," Proceedings of International Conference on Irradiation Behaviour of Metallic Materials for Fast Reactor Core Components, French Atomic Energy Commission, 1979, p. 247.

6. F. Frisius, R. Kampmann, P. A. Beaven, and R. Wagner, "Dimensional Stability and Mechanical Behaviour of Irradiated Metals and Alloys," in Proceedings of BNES Conference, Vol. 1, 1983, p. 171.

7. P. A. Beaven, F. Frisius, R. Kampmann, and R. Wagner, "SANS/TEM Studies of the Defect Microstructure of Test Reactor Irradiated Fe-Cu Alloys and Cu Containing RPV Steels," Proceedings of the 2nd International Symposium on Environmental Degradation of Materials in Nuclear Power Systems-Water Reactors, American Nuclear Society, LaGrange Park, IL, 1986, p. 400.

8. R. Wagner, F. Frisius, R. Kampmann, and P. A. Beaven, "Defect Microstructure and Irradiation Strengthening in Fe-Cu Alloys and Cu-Bearing Pressure Vessel Steels," Proceedings of 5th ASTM-Euratom Symposium on Reactor Dosimetry, Commission of the European Communities, 1984, p. 549.

9. K. C. Russell and L. M. Brown, "A Dispersion Strengthening Model Based on Differing Elastic Moduli Applied to the Fe-Cu System," Acta Metall. 20, Vol. 969, 1972.

10. S. B. Fisher, J. E. Harbottle, and N. Aldridge, "Radiation Hardening in Magnox Pressure Vessel Steels," Phil. Transactions of Royal Society of London A315, Vol. 301, 1985.

11. S. B. Fisher and J. T. Buswell, "A Model for PWR Pressure Vessel Embrittlement," International Journal of Pressure Vessel & Piping, Vol. 27, 1987 p. 91.

12. G. Solt, F. Frisius, and W. B. Waeber, "Defect Particles in an Irradiated RPV Steel Studied by Systematic Variations of Irradiation and Annealing Conditions; Preliminary Results by Small Angle Neutron Scattering," in Radiation Embrittlement of Nuclear Reactor Pressure Vessel Steels: An International Review, Vol. 3, L. E. Steele, Ed., ASTM STP 1011, American Society for Testing and Materials, Philadelphia, PA, 1989, p. 229.

13. G. Solt, F. Frisius, W. B. Waeber, and W. Buhrer, "SANS and DENS Study of Irradiation Damage in a Reactor Pressure Vessel Material with Systematic Variation of Irradiation Dose and Heat Treatments," in Effects of Radiation on Materials: 14th International Symposium, ASTM STP 1046, Vol. 2, N. H. Packan, R. E. Stolier, and A. S. Kumar, Eds., American Society for Testing and Materials, Philadelphia, PA, 1990, p. 154.

NRC FORM 335 (2-89) NRCM 1102, 3201, 3202

U.S. NUCLEAR REGULATORY COMMISSION

BIBLIOGRAPHIC DATA SHEET

(See instructions on the reverse)

1. REPORT NUMBER (Assigned by NRC, Add Vol., Supp., Rev., and Addendum Numbers, If any.)
NUREG/CR-5926
MEA-2490

2. TITLE AND SUBTITLE
SANS Investigation of Low Alloy Steels in Neutron Irradiated, Annealed, and Reirradiated Conditions

3. DATE REPORT PUBLISHED
MONTH: February
YEAR: 1993

4. FIN OR GRANT NUMBER
B5848

5. AUTHOR(S)
R. Kampmann, F. Frisius, H. Hackbarth, P. A. Beaven, R. Wagner, Institute for Materials Research, GKSS
J. R. Hawthorne, Materials Engineering Associates, Inc.

6. TYPE OF REPORT
Technical

7. PERIOD COVERED (Inclusive Dates)

8. PERFORMING ORGANIZATION – NAME AND ADDRESS (If NRC, provide Division, Office or Region, U.S. Nuclear Regulatory Commission, and mailing address; if contractor, provide name and mailing address.)

Institute for Materials Research
GKSS – Research Center
P.O. Box 1160
2054 Geesthacht, Germany

Under Contract to:
Materials Engineering Associates, Inc.
9700-B Martin Luther King, Jr. Highway
Lanham, MD 20706-1837

9. SPONSORING ORGANIZATION – NAME AND ADDRESS (If NRC, type "Same as above"; if contractor, provide NRC Division, Office or Region, U.S. Nuclear Regulatory Commission, and mailing address.)
Division of Engineering
Office of Nuclear Regulatory Research
U. S. Nuclear Regulatory Commission
Washington, D.C. 20555

10. SUPPLEMENTARY NOTES

11. ABSTRACT (200 words or less)

Small Angle Neutron Scattering (SANS) experiments were made on several low alloy steels and submerged-arc welds prototypic of nuclear reactor vessel construction. The objective was the characterization of radiation-enhanced and/or radiation-induced precipitation contributing to mechanical property changes observed in tensile and notch ductility tests of the materials. The materials were irradiated in the UBR Test Reactor under closely controlled conditions.

A portion of the samples were examined in the 288°C irradiated (I) condition; others were examined in the postirradiation annealed (IA) condition and in the 288°C reirradiated (IAR) condition. Experimental variables included material composition (primarily %Cu, %P, %Ni content), postirradiation annealing temperature (454°C and 399°C), reirradiation fluence level, and neutron-fluence rate (~0.08, 0.7, and 9×10^{12} n/cm^2-s^{-1}, E > 1 MeV). The apparent influence of the described variables on the size, number density, and composition of copper-rich precipitates was the primary focus of the SANS analyses. SANS observations are related to measured notch ductility and tensile property changes, with a view toward mechanistic explanation of the observed mechanical property trends for I, IA, and IAR conditions.

12. KEY WORDS/DESCRIPTORS (List words or phrases that will assist researchers in locating the report.)

Small Angle Neutron Scatterirg, SANS Analyses, Pressure Vessels, Low Alloy Steels, Submerged-Arc Welds, Radiation Embrittlement, Nuclear Reactors, Postirradiation Annealing, Neutron Irradiation, Reirradiation Effects, Radiation Defects, Radiation Mechanisms, Fluence-Rate Effects

13. AVAILABILITY STATEMENT
Unlimited

14. SECURITY CLASSIFICATION
(This Page)
Unclassified
(This Report)
Unclassified

15. NUMBER OF PAGES

16. PRICE

Federal Recycling Program